26th ABCM International Congress of Mechanical Engineering
November 22-26, 2021. Florianópolis, SC, Brazil

# COB-2021-1311
# MULTIDISCIPLINARY PROCEDURE FOR LOADS AND STRESS ANALYSIS OF RPA WINGS

**Ana Luiza de Souza Maran**
**Carlos Eduardo de Souza**
**Marcos Daniel de Freitas Awruch**
Mechanical Engineering Department, Aerospace Engineering
Federal University of Santa Maria, Santa Maria, RS, Brazil
analuizamaran@gmail.com, carlos.souza@ufsm.br, marcos.awruch@ufsm.br

***Abstract.*** *Remotely piloted aircraft, RPA, are showing an increasing variety of applications over the past decade. During flight, such aircraft are subjected to distributed aerodynamic loads that vary according to the operation conditions inside the flight envelope, what usually leads to the necessity of performing a large number of multidisciplinary analyses to assess the structural safety. The present study offers a procedure for coupled analysis of loads and stress on RPA wings under distributed aerodynamic loads in various critical flight conditions. All phases of a traditional static analysis are covered: the preliminary analysis, pre-processing, problem simulation and post-processing phases, respectively. A routine builds the combined envelope of gust and maneuver for prescribed mass and design velocities, identifies the critical flight conditions and distributes the aerodynamic loads on the wing. The distributed aerodynamic loads are converted to concentrated forces and applied on the Finite Element mesh, and a static solution is performed. Finally, the resulting maximum and minimum stresses computed on the structural components of the wing are evaluated according to the failure criterion of the Maximum Normal Stress for anisotropic fragile materials. The study model is an aircraft of approximately 5 kg designed for the SAE Aerodesign competition. The developed procedure showed to be an useful tool for reducing the preliminary design phase duration and improve the whole design cycle. It has already shown satisfactory results for the solution of problems related to the initial phases of the structural design of RPAs, and allows for improvement, such as coupling with optimization routines.*

***Keywords:*** *Aerodynamic loads, Finite elements, Automated procedures, Stress analysis, Wings components*

## 1. INTRODUCTION

The term Remotely Piloted Aircraft, or RPA, is applied to unmanned and remotely piloted aircraft for various purposes, except recreational. To obtain approval for its operation, all aircraft need to demonstrate certain levels of safety and reliability, and this is done based on standardized regulations for each category. The RPA must be analyzed for several specified load conditions in order to verify their structural integrity under the most adverse flight conditions. So, it is common to nominate several disciplines, each one with its responsibilities and priorities, although all essential for the full and safe functioning of the aircraft. It is a design loop, where each discipline is related to the others through a dynamic exchange of inputs and outputs, all being essential.

The loads group is the responsible for transforming various abstract data from the conceptual design phases coming from sectors such as aerodynamics, for example, into values with physical meaning for the aircraft structure. These values are then passed on as reference values for the structural design, followed by several parameter feedback in order to converge to the best results at the expense of the limitations of each sector. It is, in fact, a significantly complex and multidisciplinary process.

Finally, the developed model must be structurally evaluated to guarantee that it complies with requirements. For this purpose, the Finite Element Method (FEM), is a common tool used to analyze stresses and strains in structures under mechanical and thermal loads, in addition to carrying out sufficiently safe optimizations (Beitz *et al.*, 2007). Its creation dates back to the 50s and 60s from the studies of Turner *et al.* (1956) and Clough (1960), mainly, being the first commercial FEM software developed in 1964 (Huebner, 1975).

The automation and support to the system since the start of the engineering activities allow for reduction of delivery time and quality improvement, as well as better human resources allocation (Anderson *et al.*, 2006). It was considering this social and technological context that the Knowledge Based Engineering - KBE technique was consolidated. Acord-

ing to Quintana-Amate *et al.* (2016), the KBE method, traditionally used for improvements in engineering through the integration of software and knowledge, automation of repetitive tasks and the acceleration of processes, actually presents satisfactory results. The current FEM software allow for automation of all analysis phases through the use of scripts, for example, and is used in the present work.

The goal of the present paper is to develop a partially automated stress analysis procedure in the structural components of wings of RPAs with maximum takeoff weight (MTO) less than or equal to 25 kg designed the SAE Brasil Aerodesign competition. In order to compare the maximum stresses acting on the structural components of the wing with the established safety factor, the critical aerodynamic loads for each critical maneuver condition in the $V - n$ Diagram are surveyed. The method of structural analysis by FEM associated with an automation routine is then applied, providing an integrated design environment, very useful for partially automated preliminary structural calculations.

A brief multidisciplinary theoretical review will be presented, covering some topics of interest for the analysis of stresses in structural components of RPA wings under critical aerodynamic loading conditions. Next, the implemented framework is described and a case study is discussed.

## 2. METHODOLOGY

The basic functions of an aircraft structure are to transmit and resist applied loads, maintaining the aerodynamic shape and protecting passengers, systems and payloads from the environmental conditions encountered during the flight. The wing is one of the main structural components due to its role both in maintaining the aerodynamic forces responsible for the flight, and in supporting the internal forces arising from the action of these loads. The wing spars are subject to axial, bending, shear and torsion loads (Megson, 2017).

Computational analyzes using FEM combined with physical structural tests are performed to assess the reliability of the project. A survey of the critical aerodynamic loads that the aircraft might experience during flight is carried out, and is necessary in order to obtain the deformations and stresses in the structure. From the analysis of the maximum stresses, an adequate failure criterion for the material used must be chosen, in order to ensure the structural integrity of these components based on a given safety factor.

### 2.1 Flight Loads

During maneuvers, or in the event of gusts (turbulence), additional loads are added or subtracted from the structure of the aircraft, being measured in terms of the load factor (Niu, 2006). The load factor $n$ is a multiplier factor that defines the intensity of a load as a function of weight, and it is given by:

$$n = 1 + \frac{\Delta L}{W} \tag{1}$$

where $\Delta L$ is the lift increment and $W$ is the maximum weight of the aircraft.

The maneuvering load factor $n_{lim}$ should be treated as one that can be anticipated once during the flight, but never exceeded in a period of about 10 million flight hours (Howe, 2004), as well as the negative limiting load factor $n_{-lim}$, generally smaller than the corresponding positive factor. The ultimate positive $n_{ult}$ and negative $n_{-ult}$ load factors can be obtained by multiplying the respective positive and negative load factors, respectively, by a safety factor $SF$ (typically 1.5).

Structural load requirements are expressed in terms of some design equivalent speeds $V_0$. The stall speed $V_S$ is defined as the minimum speed at which the wing can produce enough lift to support the weight of the aircraft and maintain straight and level flight, while the maximum horizontal speed $V_H$ represent the maximum achievable speed during a straight leveled flight. The maneuvering positive $V_A$ and negative $V_{-A}$ speeds are the lowest speed at which the aircraft can reach the limit positive and negative load factor, respectively, without stalling. The cruise speed $V_C$ is defined as the minimum speed to be considered as a possible maximum speed for straight and level flight (determined so as not to exceed the maximum design speed), and the diving speed $V_D$, being the maximum structural design speed. Finally, the gust speeds *UDE* are the reference design velocities for the maximum gust intensity.

The various cases of load conditions are represented in the gust and maneuver diagram, or V-n Diagram. It is a graphic instrument used to demonstrate the structural limitations of an aircraft, defining regions, in terms of load factor and equivalent speed, where it will be able to act during the flight. Figure 1 represents the V-n Diagram, where the symmetrical dashed lines represent the linear variation of the load factor resultant when the aircraft, in a straight leveled flight ($n_{lim} = 1$), encounters a gust with speed *UDE*.

The left side of the envelope is limited by the maximum positive and negative static normal force of the aircraft. At this limit, the aerodynamic forces of the plane are in balance with the inertial forces and gravity, combined as a product of the load factor $n$ and weight $W$ (Peery and Azar, 1982). The right boundary is bounded by the maximum dive velocity $V_D$. The upper limit indicates the limit load factor expected during the flight, as a function of the aircraft's performance, for which the structural components will be dimensioned with a relative safety factor $SF$. Finally, the lower limit of the diagram, analogously to the upper one, is a indicative of the region of damage and fracture of the structure when exposed

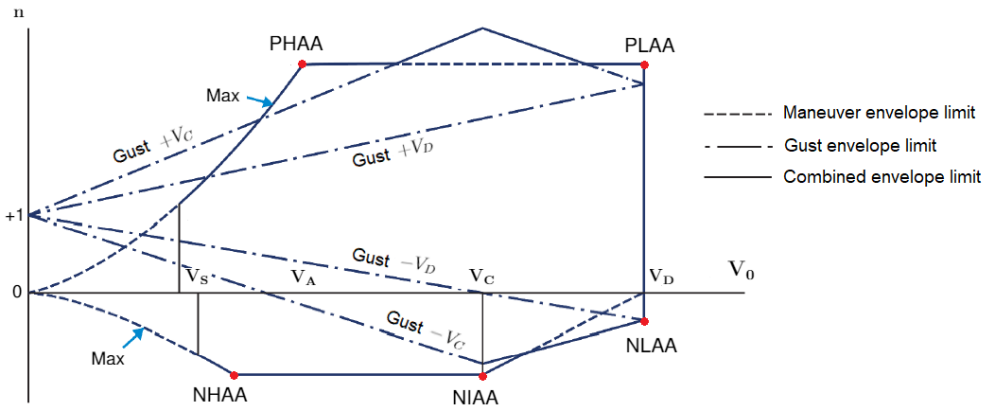


Figure 1. The V-n Diagram. Adapted from EASA (2018).

to flight conditions with negative load factors.

The structural components of the aircraft must withstand any possible combination of load factor and equivalent speed within and within the limits of the V-n Diagram. The main critical conditions are known as PHAA and PLAA under load factor $n_{lim}$ at $V_A$ and $V_D$, respectively, and NHAA and NLAA under load factor $n_{-lim}$ at $V_{-A}$ and $V_D$, respectively.

### 2.2 Aerodynamics

The computation of loads acting on wings depends on a preliminary aerodynamic study. Experimentally, the resulting aerodynamic force $R$ from the movement of the airfoil through the air depends on six variables: relative wind speed $V_\infty$, angle of attack $\alpha$, viscosity coefficient $\mu$, density of air $\rho_\infty$, velocity of sound $V_{sound}$ and reference area, or characteristic size $S$. Aerodynamic profile, or airfoil, is an aerodynamic body that, when under a certain $\alpha$, produces more lift than drag and a pitch moment (Roskam and Lan, 2000). A dimensional analysis from the six dimensional parameters $R$, $V_\infty$, $\mu$, $\rho_\infty$, $V_{sound}$ and $S$ results in three dimensionless parameters based on the Vaschy-Buckingham Theorem $\pi$ (see Anderson, 2017: p. 36), the lift $c_l$, drag $c_d$ and pitching moment $c_m$ coefficients of the airfoil.

The force $R$ can be decomposed in the aerodynamic system, obtaining the lift force $l$, perpendicular to $V_\infty$, and the drag force $d$, parallel to $V_\infty$. However, $R$ can also be decomposed relative to the body system, resulting in a normal force $F_n$ perpendicular to the chord direction and a force acting in the chord direction of the profile $F_c$ perpendicular to $F_n$. The point of action of $R$ is the place that produces the same effects as the associated distributed loads, that is, where the aerodynamic moment is null, known as the center of pressure CP (Anderson, 2017). The aerodynamic center AC is defined as the point where the moment $m_{1/4}$ around it, associated with the distance between the CP and the AC, is independent of the angle of attack.

The loads acting on the CP and AC are illustrated in Fig. 2. The center of pressure varies according to the angle of attack and is located at a distance $x_{CP}$ from the leading edge, usually after the aerodynamic center, which, in turn, is a fixed point at a distance of $c/4$ from the leading edge ($c$ is the airfoil chord).

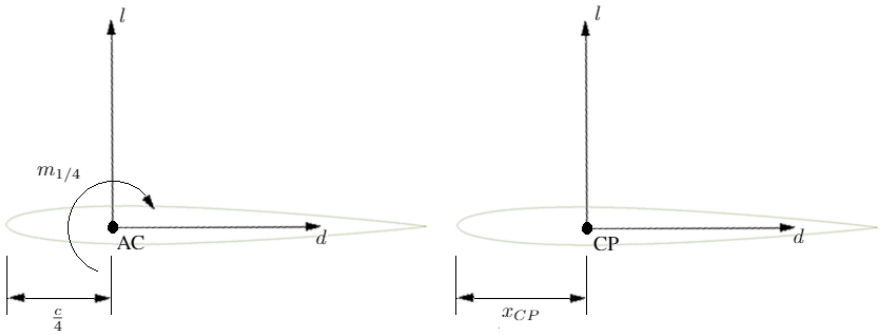


Figure 2. Aerodynamic forces acting on the $AC$, on the left, and on the CP, on the right. Adapted from Anderson (2017).

In finite wings, the load analysis is usually performed taking as reference the $AC$. The spar is usually projected directly under the $AC$, allowing for the constant pitching moment $M_{1/4}$ of a given critical condition to be anticipated in the design considerations. For finite wings, the distribution of lift $L(y)$ along the span (axis $y$) is given by the Kutta-Joukowski Theorem, which refers to a current two-dimensional irrotational fluid, at $V_\infty$ around a closed contour with circulation $\Gamma$. The lift force arises due to the aerodynamic pressure acting on the contour in a direction perpendicular to the velocity (Anderson, 2017).

The elliptical geometry is the one with the most efficient lift distribution, due to the reduction of induced drag. The lift distribution of an elliptical wing $L_E$ will be given according to the Kutta-Joukowski Theorem, varying elliptically, as well as the circulation,

$$L_E(y) = \rho_\infty V_\infty \Gamma_0 \sqrt{1 - (\frac{2y}{b})^2} \tag{2}$$

where $\Gamma_0$, which represents the maximum circulation value (obtained at the origin, $y = 0$) and $b$ is the span of the wing. However, Eq. (2) is not adequate for wings with non-elliptic geometries, in which case, the Schrenk distribution $L_S$ is often used. This distribution is obtained by taking the average between the distribution of an elliptical wing $L_E$, considered ideal, and the distribution of a trapezoidal wing $L_T$ (Schrenk, 1941),

$$L_S(y) = \frac{L_T(y) + L_E(y)}{2} \tag{3}$$

where $L_T$ is obtained by:

$$L_T(y) = \frac{2L}{(1+\lambda)b}[1 + \frac{2y}{b}(\lambda - 1)] \tag{4}$$

with $\lambda$ being the taper ratio and $L$ the total lift.

In a similar fashion, the drag distribution must be obtained. Following the methodology detailed by Roskam and Lan (2000), once the real or approximate value of $C_D$ and its distribution is known, it is then possible to calculate the drag distribution along the span as follows:

$$D(y) = q_\infty S C_D(y) \tag{5}$$

Finally, the distribution of the pitching moment $M_{1/4}$ around the aerodynamic center of the wing is obtained by:

$$M_{1/4}(y) = q_\infty S \bar{c} C_m(y) \tag{6}$$

where $\bar{c}$ is the mean aerodynamic chord.

A more precise distribution of the $C_m$, $C_D$ and $C_L$ coefficients along the span of the finite wing can be obtained by aerodynamic analysis methods of preliminary finite wings, such as the lifting line theory, the vortex lattice method and the 3D panel method.

### 2.3 Failure criterion

The prediction of safe limits for the use of materials under combination of multi-axial stresses requires the application of an adequate failure criterion. The present work considers orthotropic materials, with different strengths in different orientations. Also, brittle materials have static strength limited by their ultimate strength to fracture (either by compression or tensile). In tensile tests, brittle materials do not exhibit a well-defined yield region, generally failing after small deformations on the order of up to 5% (Dowling, 2012). The theory of maximum normal stress MNS for anisotropic brittle materials is a failure criterion that states that failure occurs whenever one or more conditions are not met. For traction, the conditions are:

$$SF_{FC} \leq \frac{\sigma_{ut_{11}}}{\sigma_{11}} \tag{7}$$

and

$$SF_{FC} \leq \frac{\sigma_{ut_{22}}}{\sigma_{22}} \tag{8}$$

where $\sigma_{11}$ and $\sigma_{22}$ are the normal stresses in the component in the principal fiber directions, and $\sigma_{ut_{11}}$ and $\sigma_{ut_{22}}$, are the ultimate tensile stresses of the material in the main fiber directions. For the plane stress case, $\sigma_{33}$ (in the direction normal to the stress plane) is zero. For compression, the conditions are:

$$SF_{FC} \geq \frac{\sigma_{uc_{11}}}{\sigma_{11}} \tag{9}$$

and

$$SF_{FC} \geq \frac{\sigma_{uc_{22}}}{\sigma_{22}} \tag{10}$$

where $\sigma_{uc_{11}}$ and $\sigma_{uc_{22}}$ are the ultimate stresses to compress the material in the main fiber directions. Finally, for shear stress, the condition is as follows:

$$SF_{FC} \leq \frac{\tau_{u_{12}}}{|\tau_{12}|} \tag{11}$$

where $\tau_{12}$ is the shear stress in the component and $\tau_{u_{12}}$ is the ultimate shear strength of the material in the plane of stresses. The factor $SF_{FC}$ is the stress safety factor established for the project based on a given failure criterion. This factor determines how far the material, under tension, is from a possible rupture.

## 3. FRAMEWORK

An overview of the procedure is given in this section. Two main branches are considered: the load cases and distributed aerodynamics loads are computed though Matlab and Python scripting and the structural analysis is performed with a CAE software.

The procedure proposed for the work is illustrated in Fig. 3. From the chosen study model, the necessary data are collected (aerodynamics, performance, model geometry, among others) for the static structural analysis in the finite element software. Most phases are automated so far, but there is still room for improvements in that sense.

The FEM software used during the static analyzes is ABAQUS/CAE, and, at the time of the project's execution, there is no known method that allows the direct assignment of distributed loads in the CAE model, except for beam elements. The solution proposed in this paper is to transform the distributed load into N concentrated loads along the half-span, where N is an input to the Matlab routine.

### 3.1 Script procedures

The Matlab routine starts by reading a .txt file containing the study model input data. Then, the V-n Diagram is built, based, as far as possible, on the CS-VLA standard. Once the V-n Diagram is constructed, the total lift load for each critical condition are obtained. Then, the coefficient $C_L$, angle $\alpha$ and total drag force for each case are calculated from the curves $C_L$ and $C_D$ already raised from the aerodynamic profile in a given Reynolds range.

The drag and lift force are expressed in s the body system, resulting in a force $F_n$ in the normal direction and another $F_c$ in the chord direction of the aerodynamic profile. The Schrenk distribution is carried out and the distributed aerodynamic loads along the span are obtained. These loads are then transformed into $N$ point loads equally spaced along the half-span.

A parallel procedure is performed in the XFLR5 preliminary aerodynamic analysis software. The objective is to obtain the distribution of the pitching moment coefficient $C_m(y)$ along the wingspan for each critical flight condition, since the Matlab routine does not yet present any method of preliminary aerodynamic analysis of finite wings. These data are fed back to the routine in Matlab, and the moment distribution along the span is calculated. The concentrated loads equivalent to the pitching moment are obtained as a moment couple acting from the same distance from the center of the stringer, in opposite directions. The two distributed loads (from opposite directions) are also replaced by $N$ concentrated loads along the half-span.

Finally, the Matlab routine creates a new Python script file, containing all the commands necessary for the automatic generation of the $N$ loads concentrated in the center and sides of the upper table of the stringer in the CAE environment. To do so, Matlab opens the Python journal file of the already made CAE model and adds new commands at the end.

The Python routine starts by creating $N$ partitions in the direction of the $x$ axis along the semi-span according to the position of the concentrated loads, and then re-meshing the span. Then, it creates a new step, the $N$ sets in the center, front and rear line in the spar cap, all the concentrated loads, boundary condition (encastre at the root of the semi-wing) and all the load cases defined by the delimiters of the V-n diagram.

### 3.2 FEM Procedures

The study model is built and analyzed from its semi-wing, for simplification purposes. The FEM software used is ABAQUS/CAE. A preliminary analysis is carried out by computing the total aerodynamic force and moment acting on the aerodynamic center in the semi-wing. These are, therefore, the expected values at the end of the static analysis in the program for the force and reaction moment of the structure, respectively, in response to the loads distributed along the half-span.

The pre-processing phase includes the modeling of the semi-wing from the definition of the types of elements, parts, materials, properties, to the point of definition of the mesh. This way, once the Python routine is reproduced, the model is ready for the solution step. When requesting a new job, the solver obtains the nodal displacements, and then computes some requested (such as stress and strain) in each element.

An appropriate failure criterion must be chosen for analyzing the results and verifying the structural integrity of the components in critical load cases. The chosen failure criterion is the maximum normal stress for anisotropic materials. The FEM model uses only shell elements, and a plane stress is considered, so that the shell normal stress is zero ($\sigma_{33} = 0$

MPa ). The stresses $\sigma_{11}$ are obtained as a function of the longitudinal direction of the fibers, while $\sigma_{22}$ are obtained as a function of the direction transverse to the fibers. The maximum normal, minimum normal, and shear stresses are evaluated based on the established design safety factor and on the ultimate tensile and compression stresses of the material used. Finally, the forces and moments of reaction of the structure in face of the applied critical loads are also compared with those predicted during the preliminary analysis phase, in order to verify if the procedures for obtaining and transforming aerodynamic loads were carried out correctly.

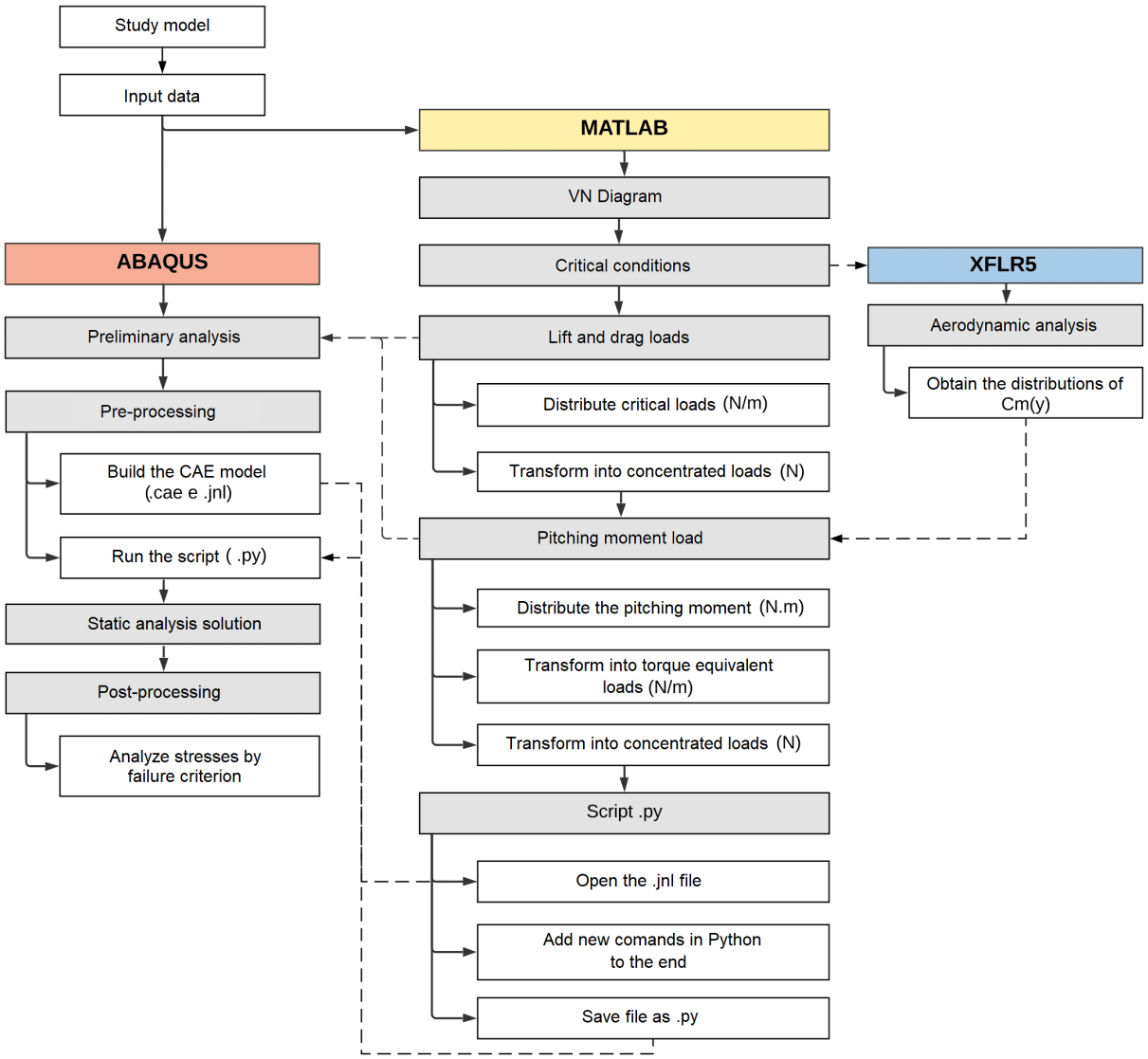


Figure 3. An overview of the complete process.

## 4. NUMERICAL STUDIES

Bandeirante, the study model chosen for the work, consists of an RPA designed and built by the Carancho Aerodesign team (UFSM) for the SAE Aerodesign competition, in 2019. The empty mass of the aircraft is approximately 1.33 kg, while the maximum payload reaches 3.27 kg. Figure 4 shows an isometric view of its CAD model. The wing frame was designed so that the center of the spar cap coincides with the aerodynamic center. The dimensions of the cross-section of the spar were estimated seeking a minimum safety factor $SF_{FC}$ of 1.5. The result was a rectangular wing with a 1.5 m span and 0,22 chord and a rectangular spar cross section of width $L_{spar} = 25$ mm and height $h_{spar} = 20$ mm (Carancho, 2019).

The material used to build the structural components of the wing is balsa wood. It is an anisotropic material, commonly used in the Aerodesign competition due to its high stress-to-weight ratio. A survey of the balsa wood properties necessary for solving, in ABAQUS/CAE, the global displacement equations in the static analysis problem, was carried out. The input data for the program are the modulus of elasticity, the Poisson's coefficient and the ultimate tensile, compression and shear strengths in the normal and parallel directions to the wood fibers. Other more specific design parameters, in

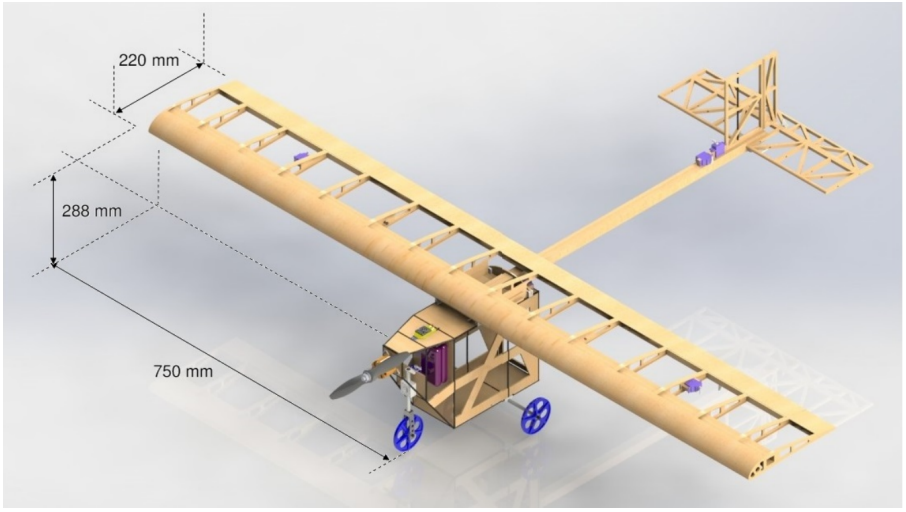


Figure 4. The aircraft model. Adapted from Carancho (2019).

addition to aerodynamic ones, were also provided by the Carancho Aerodesign team.

### 4.1 Loads and aerodynamics results

Regulations regarding RPAs, in general, do not cover the specific design requirements for their certification. Even so, it was chosen to present the CS-VLA standard from EASA (European Aviation Safety Agency) for aircraft with maximum take-off weight of up to 750 kg (EASA, 2018), even if it addresses aircraft of magnitude and purposes far from the study model. This regulation was applied, when reasonable, for the construction of the V-n Diagram.

From the maximum speed of 18 m/s taken as input data from the team, it is calculated $V_C = 15.2$ m/s, $V_S = 11.8$ m/s. The limit load factor obtained is approximately 1.5, resulting in a negative limit load factor of 0.6 (calculation made following the logic of the CS-VLA regulation). The dive velocity is calculated to be $V_D = 21.12$ m/s. The CS-VLA also addresses the equivalent burst velocities, establishing positive and negative gusts of velocity $UDE_1$ = 15.24 m/s up to $V_C$ and velocity $UDE_2$ = 7 .62 m/s $V_D$.

It is observed in Fig. 5, what gives the V-n Diagram for the study model, that, using the values stipulated by the regulation for the design speeds $UDE_1$ and $UDE_2$, the load factors of resulting gusts are quite high compared to maneuvering load factors. This is because they are estimated values for aircraft of considerably larger size and performance, capable of carrying up to two passengers, not counting the performance limitations of the study model, designed in an academic environment and with limited resources. Therefore, only the maneuver diagram (delimited by PLAA, PHAA, NLAA and NHAA points) will be considered for the analysis of critical loads.

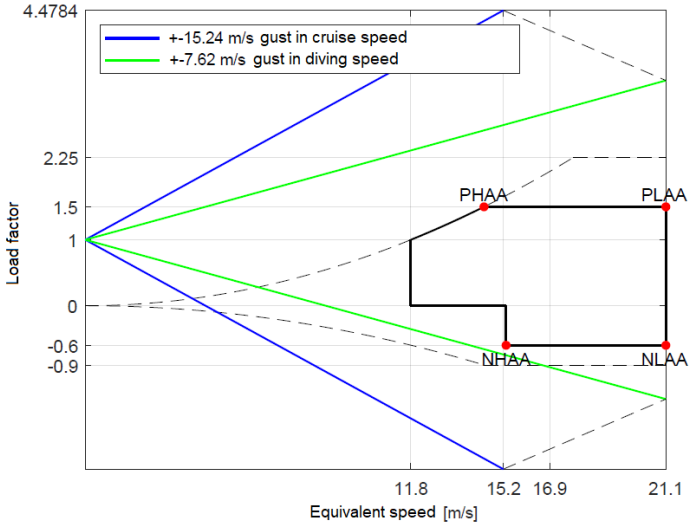


Figure 5. The V-n Diagram computed for the Bandeirante model.

Then, it is obtained the forces $L$ and $D$ in the aerodynamic system, $F_N$ and $F_C$ in the body system, the equivalent

velocities $V_0$ and the angles of attack $\alpha$ values for each of the four critical cases. The total loads acting on the body system are distributed by Schrenk's method for each condition, and finally replaced by $N = 100$ concentrated forces acting along the half-span. The pitching moment distribution along the semi-span is obtained from the distribution of the coefficient $C_m(y)$ extracted from the XFLR5 software for each combination of velocity and angle of attack of each critical condition. The moment $M_{1/4}$ is replaced by a couple of forces that have the same effect on the spar, acting at a distance $L_{long}/2 = 12.5$ mm.

### 4.2 FEM Results

A preliminary analysis is performed to obtain the reaction values expected from the structure, $F_N/2$ and $F_C/2$, in the body system, as well as the moment $M_{1/4}/2$ acting around the $y$ axis. The forces and moments are divided in half as they correspond to the loads of the semi-wing modeled in ABAQUS/CAE, and not the entire model.

Moving on to the pre-processing phase, the right semi-wing of Bandeirante is modeled in the ABAQUS/CAE environment. It is composed of nine ribs and one spar of a 3 mm balsa wood shell, and a aileron, leading and trailing leading edges of 1,5 mm balsa wood shell.

The Python routine is then reproduced, after the initial modeling and definition of material properties. Figure 6 represents the CAE model at the end of the pre-processing phase, with the loads and boundary condition of the PLAA case (as an example) applied. It is noteworthy that all concentrated loads are represented by vectors of the same magnitude, even if different, in practice.

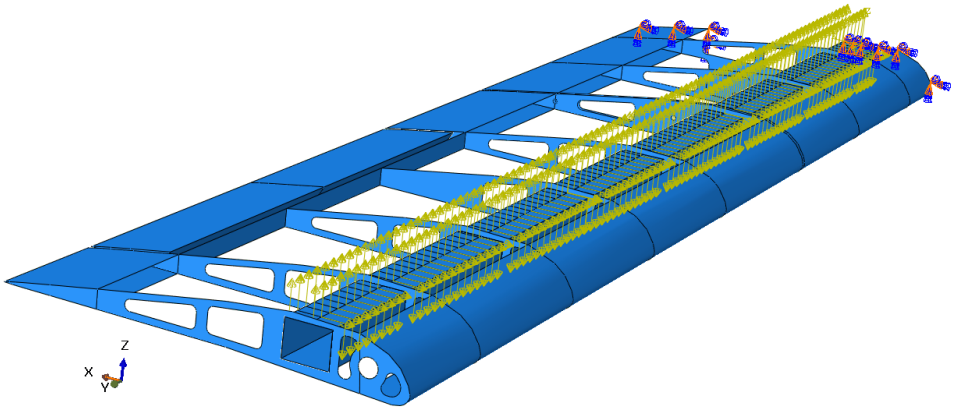


Figure 6. Loads and boundary conditions.

In order to obtain principal stress results from displacements along the structure, a static analysis is performed. Table 1 presents the main results obtained for the four critical load cases, including the maximum and minimum stresses $\sigma_{11}$, $\sigma_{22}$ and $\tau_{12}$, in addition to the maximum displacements at the tip of the wing.

Table 1. Main results from static analysis.

| **Results** | **PLAA** | **PHAA** |
|---|---|---|
| $\sigma_{\mathbf{11_{max}}}$ $(\mathbf{SF_{FC}})$ | 5.68 MPa (2.87) | 5.42 MPa (3.01) |
| $\sigma_{\mathbf{22_{max}}}$ $(\mathbf{SF_{FC}})$ | 0.23 MPa (3.56) | 0.16 MPa (5.12) |
| $\tau_{\mathbf{12_{max}}}$ $(\mathbf{SF_{FC}})$ | 0.44 MPa (4.93) | 0.28 MPa (7.75) |
| $\lvert\sigma_{\mathbf{11_{min}}}\rvert$ $(\mathbf{SF_{FC}})$ | 8.56 MPa (1.25) | 6.89 MPa (1.55) |
| $\lvert\sigma_{\mathbf{22_{min}}}\rvert$ $(\mathbf{SF_{FC}})$ | 0.21 MPa (3.38) | 0.16 MPa (4.44) |
| $\lvert\tau_{\mathbf{12_{min}}}\rvert$ $(\mathbf{SF_{FC}})$ | 0.61 MPa (3.55) | 0.43 MPa (5.05) |
| Max. displacements at the wing tip | 32.75 mm | 25.29 mm |
| **Results** | **NLAA** | **NHAA** |
| $\sigma_{\mathbf{11_{max}}}$ $(\mathbf{SF_{FC}})$ | 4.67 MPa (3.49) | 3.5 MPa (4.66) |
| $\sigma_{\mathbf{22_{max}}}$ $(\mathbf{SF_{FC}})$ | 0.18 MPa (4.55) | 0.01 MPa (82) |
| $\tau_{\mathbf{12_{max}}}$ $(\mathbf{SF_{FC}})$ | 0.45 MPa (4.82) | 0.24 MPa (9.04) |
| $\lvert\sigma_{\mathbf{11_{min}}}\rvert$ $(\mathbf{SF_{FC}})$ | 3.72 MPa (2.88) | 2.38 MPa (4.51) |
| $\lvert\sigma_{\mathbf{22_{min}}}\rvert$ $(\mathbf{SF_{FC}})$ | 0.22 MPa (3.22) | 0.12 MPa (5.92) |
| $\lvert\tau_{\mathbf{12_{min}}}\rvert$ $(\mathbf{SF_{FC}})$ | 0.44 MPa (4.93) | 0.24 MPa (9.04) |
| Max. displacements at the wing tip | 9.56 mm | 7.86 mm |

The maximum displacement at the tip of the wing is approximately 3.3 cm, which is a very common result for

the context of the study model's performance in Aerodesign. It is noticed, also, that the safety factor for the PLAA case did not reach the minimum safety factor established for the project in all situations of maximum absolute stress ($SF_{FC} = 1.25 \leq 1.5$). Therefore, changes are needed in the structural design according to the analysis here performed, in order to increase its strength and ensure structural integrity according to the established criteria.

In this case, a solution can be obtained by reinforcing the spar with glass fibers, since it is the place of critical compressive stresses. The lamination process, usually carried out in vacuum, tends to significantly increase the ultimate stresses $\sigma_{uc}$ and $\sigma_{ut}$ of balsa wood and is already a very popular tactic among Aerodesign teams. It is also possible to change the thickness of its shells, or to design a variable cross-section spar reinforced only in the regions of greater stress, close to the root.

In addition, the forces and reaction moments resulting from the static analysis in ABAQUS/CAE are evaluated, in order to verify the efficiency of the proposed procedure in this work. Table 2 presents the final values of the reactions of the semi-wing structure under the critical aerodynamic loads compared with those predicted during the preliminary analysis for all critical conditions.

Table 2. Comparison between the final reaction forces and moments of the structure with those previously predicted.

| Condition | $M_{1/4}/2$ Predicted/Final | $F_N/2$ Predicted/Final | $F_C/2$ Predicted/Final |
|---|---|---|---|
| PLAA | 1.05 / 1.42 N.m | -33.88 / -34.57 N | 0.33 / 0.33 N |
| PHAA | 0.44 / 0.59 N.m | -33.51 / -34.52 N | 5.86 / 6.08 N |
| NLAA | 1.24 / 1.68 N.m | 13.54 / 13.82 N | 0.75 / 0.76 N |
| NHAA | 0.68 / 0.92 N.m | 13.49 / 13.77 N | 1.28 / 1.31 N |

It is noticed that the final reaction values of the structure are very close to the expected values. Some factors that can influence this small difference in results include the transformation of distributed loads by the Schrenk method to concentrated loads, which is performed from several approximations, as well as the Schrenk distribution itself, which is an approximation used only in early stages of project. Furthermore, the distributions of $M_{1/4}$, in general, have a lot of curves, making the approximation to a polynomial a little less efficient (even if it is of high order).

Lastly, it should be noted that the pitching moment estimated initially as a reaction of the structure is an approximation, considering that it was also obtained by integrating the curve formed by the numerous points provided by the XFLR5.

## 5. CONCLUDING REMARKS

In the present work, a semi-automate procedure for loads and stress of structural components of RPAs wings was presented. The methodology was applied to a wing previously designed for the Aerodesign competition. The flight envelope was defined in terms of a V-n Diagram. At the critical points, distributed aerodynamic loads were computed. The distributed aerodynamic loads are transformed to concentrated forces, applied at an arbitrary number of points, which can be adjusted based on a convergence analysis. A failure criteria adequate to anisotropic material was considered, and it was observed that the safety factor lies above the minimum required at one point of the flight envelope (PLAA condition). The procedure showed to be adequate to identify a critical structural element and indicate a local change in the design.

The developed procedure constitutes a useful academic structural analysis tool that can be greatly improved in order to maximize its potential. For future work, it is intended to add a preliminary aerodynamic analysis procedure to the Matlab routine and eliminate the dependence on external software, such as XFLR5. However, before it, it is recommended to rewrite the whole Matlab routine itself in Python, focusing on a single (and essential, considering the ABAQUS/CAE automated routine phase) programming language. Finally, it would be useful to add to the wing analysis the effects of other loads (such as the contact load from the attachment between the center section and the fuselage, for example), as well as to develop new procedures for stress analysis on the other structural components of RPAs, such as vertical and horizontal stabilizer, fuselage and landing gear.

## 6. REFERENCES

Anderson, J.D., 2017. *Fundamentals of aerodynamics*. McGraw-Hill series in aeronautical and aerospace engineering. McGraw Hill Education, 6th edition.

Anderson, P., Efstrom, B.O. and Boart, P., 2006. "Knowledge enabled pre-processing for structural analysis". *1st Nordic Conference on Product Lifecycle Management*, pp. 89–97.

Beitz, W., Feldhusen, J., Grote, K.H. and Pahl, G., 2007. *Engineering Design: A systematic Approach*. Springer, 3rd edition.

Carancho, 2019. *Relatório de Estruturas e Ensaios Estruturais*. Carancho Aerodesign.

Clough, R.W., 1960. "The finite element method in plane stress analysis". *2nd Conference on Electronic Computation*.

Dowling, N.E., 2012. *Mechanical Behavior of Materials*. Prentice Hall, 4th edition.

EASA, 2018. *Easy Access Rules for Very Light Aeroplanes*. European Aviation Safety Agency.

Howe, D., 2004. *Aircraft Loading and Structural Layout*. The Aerospace Series. Professional Engineering Publishing Limited.

Huebner, K.H., 1975. *The Finite Element Method for Engineers*. John Wiley & Sons, 1st edition.

Megson, T.H.G., 2017. *Aircraft Structures for Engineering Students*. Elsevier Aerospace Engineering Series. Butterworth-Heinemann, 6th edition.

Niu, M.C.Y., 2006. *Airframe Structural Design: Practical Design Information and Data on Aircraft Structures*. Adaso Adastra Engineering Center, 2nd edition.

Peery, D.J. and Azar, J.J., 1982. *Aircraft Structures, 2nd Ed.* McGraw-Hill Book Company, New York, 2nd edition.

Quintana-Amate, S., Bermell-Garcia, P., Tiwari, A. and Turner, C.J., 2016. "A new knowledge sourcing framework for knowledge-based engineering: An aerospace industry case study". *Computers & Industrial Engineering*, Vol. 34, pp. 35–50.

Roskam, J. and Lan, C.T., 2000. *Airplane Aerodynamics and Performance*. Darcorporation, revised edition.

Schrenk, O., 1941. "A simple approximation method for obtaining the spanwise lift distribution." *The Aeronautical Journal*, Vol. 45, No. 370, pp. 331–336.

Turner, M.J., Clough, R.W., Martin, H.C. and Topp, L.J., 1956. "Stiffness and deflection analysis of complex structures". *Journal of the Aeronautical Sciences*.

## 7. RESPONSIBILITY NOTICE

The author(s) is (are) solely responsible for the printed material included in this paper.